Creating a dry variety of quicksand

4 authors, including:

D. Lohse
University of Twente
1,138 PUBLICATIONS   **40,467** CITATIONS

SEE PROFILE

Devaraj van der Meer
University of Twente
200 PUBLICATIONS   **3,684** CITATIONS

SEE PROFILE

Some of the authors of this publication are also working on these related projects:

Fluid Dynamics of Infectious Diseases View project

Solidification of Droplets View project

Creating a dry variety of quicksand

An aerated form of sand engulfs objects instantaneously, shooting out a jet of grains.

Sand can normally support a weight by relying on internal force chains[1–3]. Here we weaken this force-chain structure in very fine sand by allowing air to flow through it: we find that the sand can then no longer support weight, even when the air is turned off and the bed has settled — a ball sinks into the sand to a depth of about five diameters. The final depth of the ball scales linearly with its mass and, above a threshold mass, a jet is formed that shoots sand violently into the air.

We allowed air to flow through very fine sand (typical grain diameter was about 40 μm), which was sitting in a container with a perforated base. The air stream was turned off before the start of the experiment and the sand allowed to settle (see supplementary information for details of methods). The packing fraction of this sand was only 41%, compared with 55–60% for untreated sand. We call this fragile state of sand 'dry quicksand' (not to be confused with normal quicksand, which is a mixture of sand, clay and water).

A ping-pong ball of radius $R = 2.0$ cm, partly filled with bronze grains, was suspended above the treated sand so that it was just touching the surface. To release the ball without introducing any vibration, the thin rope supporting the ball was burned — causing the ball to sink instantaneously into the sand (Fig. 1). Objects often make a splash when they hit sand[4,5]; in this case there was no splash, as expected, but a straight jet of sand shot violently into the air after about 100 ms[4,5]. The singularity leading to this jet formation has already been described[5].

In experiments using a ball that has a stiff, almost mass-less tail, which allows for tracking of the sinking depth as a function of time, we find that the ball reaches a final depth of $z_{final} = 22.4$ cm (Fig. 2). This corresponds to more than five times its diameter. We investigated how this phenomenon is affected by the mass of the ball and found that the final depth reached by the ball increases linearly with its mass: that is, $z_{final} \propto m$. A visible jet only develops beyond a threshold mass of $m_{thres} = 28.5$ g (Fig. 2).

We developed a simple force model to describe the dynamics of the ball in the sand and the parameter dependence of the final depth. The ball is accelerated by gravity and at the same time experiences a drag force, F_D, from the sand grains. For simplicity, we assume a Coulomb drag due to the normal forces from the side, which increases linearly with the depth z (ref. 6); pressure saturation due to sidewall support (Rayleigh–Janssen law) occurs only at much greater depth. We therefore have $F_D = -\kappa z$, where κ is a
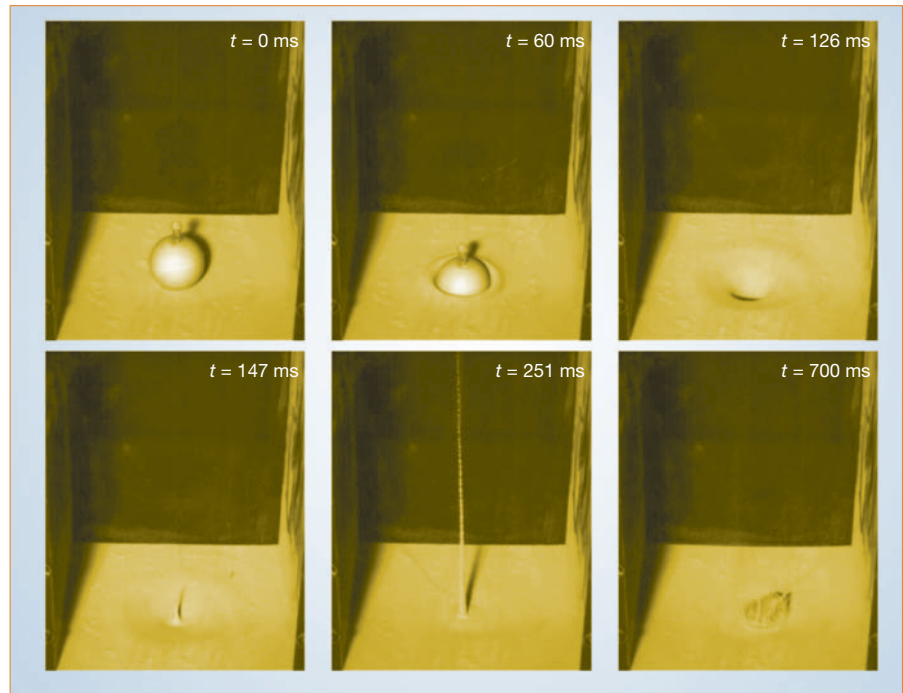

Figure 1 Snapshots of the sinking-ball experiment. At time $t = 0$ ms, the ball (mass $m = 133$ g) is released and immediately starts to sink into the sand; at $t \approx 130$ ms, a sand jet emerges, which reaches its final height at $t \approx 180$ ms. After about 600 ms, the trapped air bubble reaches the surface. (Experiment was built with assistance from G. W. Bruggert and input from C. Drösser.)

constant; note that F_D does not depend on velocity. The equation of motion is thus

$$(m + m_A)\ddot{z} = mg - \kappa z \qquad (1)$$

where m_A is the 'added mass', meaning the mass of sand that is accelerated along with the moving ball. Equation (1) has to be supplemented by the boundary conditions $z(0) = 0$ and $\dot{z}(0) = 0$. Integration of equation (1) immediately gives the final depth,

Figure 2 The jet height, h_{jet} (red circles), and the final depth of the ball, z_{final} (blue diamonds), as functions of the ball mass, m. Blue dashed line, linear fit with slope $2g/\kappa$; red dotted line, fit $h_{jet} \propto (m - m_{thres})^{1.0}$. The ball is released from rest from the surface of the sand (Fig. 1). Inset, depth of the ball, z, as function of time, t, for a ball of mass 148 g (experiment: blue curve; model: red curve).

$z_{final} = 2mg/\kappa$: that is, depth depends linearly on the mass. This agrees with the experimental findings shown in Fig. 2, from which we can read off $\kappa = 13.3 \pm 0.5$ N m^{-1}. The full solution of equation (1) is

$$z(t) = \frac{1}{2} z_{final}(1 - \cos(\omega t)) \qquad (2)$$

for $0 \le t \le \pi/\omega$, where $\omega = \sqrt{\kappa/(m + m_A)}$. Equation (2) describes the dynamics extremely well (Fig. 2, inset). From the fitted ω, we obtain m_A as zero, within measurement precision.

In nature, dry quicksands may evolve from the sedimentation of very fine sand after it has been blown into the air and, if large enough, might be a threat to humans. Indeed, reports that travellers and whole vehicles have been swallowed instantly[7,8] may even turn out to be credible in the light of our results.

Detlef Lohse, Remco Rauhé, Raymond Bergmann, Devaraj van der Meer
Faculty of Science and J.M. Burgers Centre for Fluid Dynamics, University of Twente, 7500 AE Enschede, The Netherlands
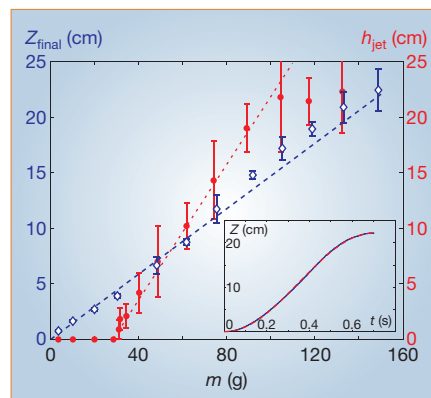*e-mail: d.lohse@utwente.nl*

1. Liu, C. H. *et al. Science* **269,** 513 (1995).
2. Jaeger, H. M., Nagel, S. R. & Behringer, R. P. *Phys. Today* **49,** 32–38 (1996).
3. Snoeijer, J. H., Vlugth, T. J. H., van Hecke, M. & van Saarloos, W. *Phys. Rev. Lett.* **92,** 054302 (2004).
4. Thoroddsen, S. T. & Shen, A. Q. *Phys. Fluids* **13,** 4–7 (2001).

5. Lohse, D. *et al. Phys. Rev. Lett.* **93**, 198003 (2004).
6. Stone, M. B. *et al. Nature* **427**, 503–504 (2004).
7. Lawrence, T. E. *Seven Pillars of Wisdom* (Anchor, New York, 1926).
8. Bagnold, R. A. *The Physics of Blown Sand and Desert Dunes* (Methuen, London, 1941).

Supplementary information accompanies this communication on *Nature*'s website.

Competing financial interests: declared none.

Adhesion

Elastocapillary coalescence in wet hair

We investigated why wet hair clumps into bundles by dunking a model brush of parallel elastic lamellae into a perfectly wetting liquid. As the brush is withdrawn, pairs of bundles aggregate successively, forming complex hierarchical patterns that depend on a balance between capillary forces and the elasticity of the lamellae. This capillary-driven self-assembly of flexible structures, which occurs in the tarsi of insects[1] and in biomimetic adhesives[2] but which can also damage microelectromechanical structures[3–6] or carbon nanotube 'carpets'[6–8], represents a new type of coalescence process.

When the brush, which consists of regularly spaced, flexible lamellae, is progressively withdrawn from the bath of liquid, a cascade of successive sticking events leads to a hierarchical bundling pattern (Fig. 1a). We studied one such elementary sticking event for two lamellae separated by a distance d. If the strips were rigid, the perfectly wetting liquid would rise up to Jurin's height, $h_J = 2L_C^2/d$, where $L_C = (\gamma/\rho g)^{1/2}$ is the capillary length; γ and ρ are the liquid's surface tension and density, respectively. When the strips are flexible, capillary suction bends the lamellae and the liquid rises higher in this more confined environment. As two lamellae are withdrawn to height L (Fig. 1b), a capillary rise to height h_J (or to the top when $L < h_J$) precedes the sticking together of the strips, which happens when L becomes large.

Surprisingly, the height of rise L_{wet} increases linearly with L in this last regime, whereas $L_{dry} = L − L_{wet}$ remains constant. In fact, L_{dry} is prescribed by a balance between capillarity and elasticity. The capillary energy (per unit width) is $−2\gamma L_{wet}$, whereas the elastic energy is proportional to the square of the typical curvature, d/L_{dry}^2, and reads exactly $3\kappa d^2/L_{dry}^3$ in this geometry, where κ is the bending stiffness of the strips. Minimizing the sum of the two energies (gravity becomes negligible in this regime) with respect to L_{dry} yields

$$L_{dry}^4 = \frac{9}{2} d^2 L_{EC}^2 \qquad (1)$$

where $L_{EC} = (\kappa/g)^{1/2}$ is the elastocapillary length, in agreement with measurements made over several orders of magnitude
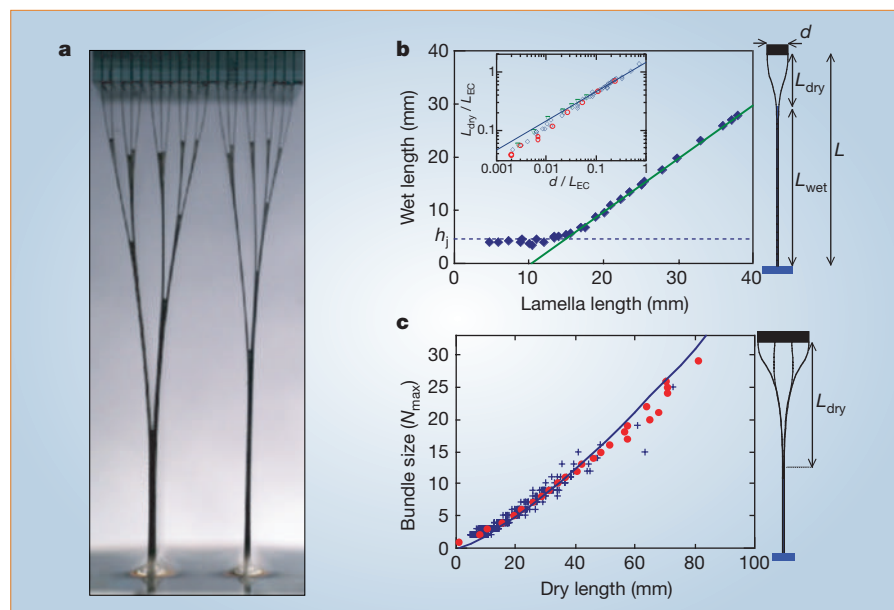

Figure 1 Flexible lamellae stick together after wetting. **a,** Lamellae in a wetted model brush after a sequence of sticking or unsticking events that cause aggregation (viewing from top to bottom) or fragmentation (from bottom to top), respectively. **b,** Height of rise, L_{wet}, of liquid between a lamella pair is plotted against the withdrawal height, L, showing the transition from the capillary rise (dashed line; $L_{wet} = h_J$) to the sticking regime (full green line; $L_{dry} = L − L_{wet}$ is constant). Polyester strips separated by $d = 1$ mm (width, 25 mm; thickness, $e = 100$ μm; bending rigidity, $\kappa = 5.1 \times 10^{-4}$ N m) were dipped into silicon oil (density, $\rho = 950$ kg m^{-3} and surface tension $\gamma = 20.6$ mN m^{-1}, leading to $h_J = 4.3$ mm). Inset, sticking regime. Non-dimensional dry length, L_{dry}/L_{EC}, is plotted against non-dimensional separation, d/L_{EC}; $L_{EC} = (\kappa/\gamma)^{1/2}$ is the elastocapillary length (red circles: $e = 50$ μm, $L_{EC} = 47$ mm; blue diamonds: $e = 100$ μm, $L_{EC} = 150$ mm; green triangles: $e = 170$ μm, $L_{EC} = 370$ mm; line: comparison with theory (equation (1); no adjustable parameter). **c,** Aggregation of multiple lamellae into bundles ($e = 50$ μm, $d = 1$ mm). Number of lamellae per bundle is plotted against dry length. Blue crosses, raw data; red circles, averaging of data; line, comparison with theory (equation (2); no adjustable parameter).

(Fig. 1b, inset). An identical energy formulation is found in fracture theory[9], in which the capillary energy is replaced by the material fracture energy. Whereas L_{EC} gives the typical curvature induced by capillarity[10], L_{dry} is the critical length above which lamellar structures collapse. When the dimensions of a structure are scaled down by a factor λ, both L_{EC} and L_{dry} (scaling as $\lambda^{3/2}$ and $\lambda^{5/4}$, respectively) eventually become smaller than the structure size, an effect that is responsible for damaging microsystem structures[2–8].

To generalize equation (1) to multiple lamellae, we assume that a cluster of N lamellae behaves as a single lamella that is N times more rigid (we neglect solid friction as the wetting liquid lubricates the strips). On average, such a cluster results from the self-similar aggregation of two bundles of size $N/2$, clamped at a distance $Nd/2$. The dry length (above the junction of the two clumps) becomes

$$L_{dry}^4 = \frac{9}{16} N^3 d^2 L_{EC}^2 \qquad (2)$$

which is in good agreement with experiment (Fig. 1c). The maximum size N_{max} of clusters in a brush with lamellae of length L is given by equation (2), with $L_{dry} = L$. However, smaller bundles are also seen if their aggregation with a neighbour leads to a size exceeding N_{max}. The broad distribution of clump sizes results from random initial imperfections, and requires statistical analysis. A derivation based on Smoluchowski's coalescence process[11] leads to an original self-similar distribution that predicts an average cluster size of $0.67N_{max}$ (A. B. *et al.*, manuscript in preparation).

Our results, once scaled down, could help to improve the design of micro-electromechanical systems. The self-similar aggregation process described here should extend to different geometries (such as those of fibrous materials) and to similar systems involving coalescence or fragmentation.

José Bico*, Benoît Roman*, Loïc Moulin*, Arezki Boudaoud†

**Physique et Mécanique des Milieux Hétérogènes (UMR CNRS 7636), ESPCI, and †Laboratoire de Physique Statistique de l'ENS (UMR CNRS 8550), 75231 Paris Cedex 5, France*
e-mail: jbico@pmmh.espci.fr

1. Eisner, T. & Aneshansley, D. J. *Proc. Natl Acad. Sci. USA* **97**, 6568–6573 (2000).
2. Geim, A. *et al. Nature Mater.* **2**, 461–463 (2003).
3. Tanaka, T., Morigami, M. & Atoda, N. *Jpn. J. Appl. Phys.* **32**, 6059–6064 (1993).
4. Mastrangelo, C. H. & Hsu, C. H. *J. Microelectromech. Syst.* **2**, 33–55 (1993).
5. Raccurt, O., Tardif, F., Arnaud d'Avitaya, F. & Vareine, T. *J. Microelectromech. Syst.* **14**, 1083–1090 (2004).
6. Hui, C. Y., Jagota, A., Lin, Y. Y. & Kramer, E. J. *Langmuir* **18**, 1394–1407 (2002).
7. Lau, K. *et al. Nano Lett.* **3**, 1701–1705 (2003).
8. Chakrapani, N., Wei, B., Carrillo, A., Ajayan, P. M. & Kane, R. S. *Proc. Natl Acad. Sci. USA* **101**, 4009–4012 (2004).
9. Freund, L. B. *Dynamic Fracture Mechanics* (Cambridge Univ. Press, Cambridge, 1990).
10. Cohen, A. E. & Mahadevan, L. *Proc. Natl Acad. Sci. USA* **100**, 12141–12146 (2003).
11. Leyvraz, F. *Phys. Rep.* **383**, 95–212 (2003).

Competing financial interests: declared none.